



ANALYTICAL SOLUTION OF CONVECTIVE DRYING OF THIN APPLE SLICES WITH MICROWAVE PRE-TREATMENT

Georgios Xanthopoulos^{1*}, Diamanto Lentzou¹, Ećim-Đurić Olivera²,
Milanović P. Mihailo²

¹Agricultural University of Athens, Department of Natural Resources Management, and
Agricultural Engineering, Athens, Greece

²University of Belgrade, Faculty of Agriculture, Zemun-Belgrade, Serbia

*Corresponding author: xanthopoulos@aua.gr (G. Xanthopoulos)

Abstract. The aim of this study was to experimentally investigate the drying characteristics of Idared apple thin discs (slices) during convective drying with microwave (MW) pre-treatment and to develop analytical modeling for thin-layer convective drying of apple slices. The drying experiments were carried out in laboratory-scale hot-air dryer using apple discs of 2 mm thickness at a drying temperature of 50 °C. The air velocity during all experiments was maintained at 2 m/s. MW pre-treatments were applied in a microwave oven operating at 700 W, with exposure times of 1 min, and 3 min. For each experiment, the drying time and equilibrium moisture content were determined. Analysis of drying curves showed that MW pre-treatment significantly reduced the overall drying time.

Keywords: apple slices, convective drying, MW, analytical solution

1. INTRODUCTION

Drying is one of the principal unit operations in food and postharvest processing, employed to reduce moisture content, inhibit microbial growth, and extend shelf life [1], [2]. In thin-layer drying of fruit slices such as apples, controlling drying kinetics while preserving product quality is a persistent challenge. Convective hot air drying remains widely used owing to its simplicity and scalability, but its slow rates and potential quality degradation increase interest in pre-treatments that accelerate moisture removal [3].

Microwave pre-treatment is a promising approach, because microwave energy penetrates the sample, generating internal heating and vapor pressure that can enhance moisture diffusive fluxes [2]. Several studies report that combining convective drying with microwave or microwave-assisted steps reduces drying time significantly compared to convection alone [1], [2], [3], [4]. In apple slices, for example, microwave-vacuum pre-treatments have been shown to reduce drying time by 25–45% versus untreated slices [5], [6]. However, the application of microwaves may also accelerate undesirable changes (e.g. surface hardening, quality deterioration) unless well integrated into a modeling framework that accounts for evolving transport properties.

Mechanistic modeling of drying processes is crucial for predictive design, process optimization, and scale-up. Classical approaches treat drying as unsteady diffusion through



the material, often applying Fick's second law with convective boundary conditions [7]. In fruit drying, effective moisture diffusivity (D_{eff}) and surface mass transfer coefficient (k_c) are key parameters, typically estimated by fitting models to experimental moisture ratio (MR) data [8]. While many models assume constant diffusivity, recent work suggests that transport properties may evolve due to structural changes (e.g. porosity variation, shrinkage) during drying [9], [10]. Time-dependent or moisture-dependent parameter formulations can better capture such dynamics but at the cost of additional complexity and potential parameter identifiability issues [11], [12], [13].

In this study, we focus on thin discs (2 mm) of *Idared* apple variety subjected to convective drying at 50 °C, with or without microwave pre-treatment (1 min, and 3 min exposure). Our aims are twofold: (i) to experimentally characterize and compare drying kinetics under the different pre-treatment regimes, and (ii) to develop and validate an analytical modeling framework that uses a constant D_{eff} paired with a time-varying k_c , thus balancing economy and mechanistic interpretability. The resulting model can help elucidate the role of internal diffusion versus surface resistance in thin fruit slices and guide the design of efficient drying protocols.

2. THEORY

2.1. Analytical solution of moisture diffusion in slab geometry

Drying of biological products is primarily governed by unsteady-state moisture transport, which is often described by *Fick's second law of diffusion* [7]. For apple slices where the thickness (L) is much smaller than the radius ($L \ll R$), the geometry can be approximated as a *thin disk*. In this case, axial diffusion across the thickness dominates, whereas radial diffusion can be neglected.

For isotropic and homogeneous media, the one-dimensional (1-D) diffusion equation is expressed as,

$$\frac{\partial M}{\partial t} = D_{eff} \frac{\partial^2 M}{\partial x^2}, \quad 0 \leq x \leq L \quad (1)$$

where D_{eff} is the effective moisture diffusivity, (m^2/s), M is the local moisture content (kg_w/kg_{dm}) at position x and time t , and x is the distance from the mid-plane (0 at the center, L at the surface). The initial condition assumes a uniform moisture distribution, $M(x, 0) = M_0$. At the surfaces, convective mass transfer to air is described by a *Robin-type* boundary condition:

$$-D_{eff} \frac{\partial M}{\partial x} \Big|_{x=L} = k_c (M_s - M_\infty), \quad (2)$$

where k_c is the convective mass transfer coefficient (m/s), M_s is the surface moisture content, and M_∞ is the equilibrium value. Symmetry is imposed at the mid-plane, ($\partial M / \partial x |_{x=0} = 0$). In this formulation, the moisture flux boundary condition is applied to



both flat faces of the slab. For long drying times or small Biot numbers, the analytical solution for a plane slab [7] simplifies to:

$$\mathbf{MR} \approx \frac{\mathbf{8}}{\pi^2} \exp\left(-\frac{\pi^2 D_{eff} t}{4L^2}\right) \quad (3)$$

This first-term approximation is valid when $t > 0.2L^2/D_{eff}$, as higher-order terms decay exponentially faster. The average moisture content can be obtained by integration across the slab thickness, $M(t) = \frac{1}{L} \int_0^L M(x, t) dx$. In practice, model fitting to experimental moisture data is performed by nonlinear regression, simultaneously estimating D_{eff} and k_c . The quality of the model fit is evaluated using root mean square error (RMSE) and the adjusted coefficient of determination R_{adj}^2 .

2.2 Justification of the slab geometry assumption (axial vs. radial diffusion, Biot numbers)

The dominance of axial diffusion in apple slices can be demonstrated by comparing characteristic surface areas and diffusion times. The total area of the two flat faces is $A_{faces} \approx 2\pi R^2$, whereas the curved side area is $A_{side} \approx 2\pi RL$. For a 2 mm-thick slice with initial radius of 0.0375 m, the side area accounts for only about 5% of the total surface, indicating that most moisture transfer occurs through the faces. Characteristic diffusion times are defined as $\tau_z = D_{eff} t_f / L^2$ and $\tau_r = D_{eff} t_r / R^2$ with $D_{eff} \approx 10^{-6}$ m²/s, $L = 0.001$ m, and $t_f \approx 13,000$ s, the axial diffusion time ($\tau_z \approx 10$) indicates essentially complete moisture equilibration across the thickness, whereas radial diffusion ($\tau_r \approx 10^{-2}$) is negligible. Thus, moisture gradients across the thickness dominate, validating the use of the slab (1-D axial) model for drying of apple slices.

2.3 Internal vs. external resistances and Biot number

The relative importance of internal and external resistances is quantified by the Biot number defined as $Bi = k_c L / D_{eff}$. When $Bi \gg 1$, internal diffusion dominates; when $Bi \ll 1$, external mass transfer dominates. For apple slices dried at 50 °C, estimated Biot numbers are very small (10^{-4} - 10^{-3}), confirming that internal diffusion is the rate-limiting step, whereas surface resistance plays only a minor role. This theoretical framework underpins the modeling approach used in this work, where D_{eff} represents the internal diffusion process and k_c captures external resistance effects, which may vary with drying time due to evolving surface structure microstructure.

3. MATERIALS AND METHODS

3.1 Preparation of apple slices

Fresh Idared apples were used in all experiments. The apples were washed with tap water, before being cut into thin circular slices. The initial geometry of the slices was



as follows: thickness ($2L$)=0.002 m ($L=0.001$ m, representing the half-thickness used in modeling). The average initial diameter was 0.075m (corresponding to an initial radius $R\approx 0.0375$ m), which gradually decreased to approximately 0.055 m after drying (average $R\approx 0.0275$ m). These dimensions were used in the calculation of effective surface area and characteristic diffusion times. The mass of the samples was 86.48 g, 65.51 g, and 76.22 g for convective, 1 min and 3 min convective drying with microwave pre-treatment, respectively. The precision balance used in the experiments was KERN & Sohn, KB 3600-2N with the accuracy of ± 0.01 g. The experiments were done only once. The ambient relative humidity was not controlled or recorded, but it was measured with digital hygrometer and it was between 55-60% during the experiments.

3.2 Drying experiments

Convective drying was carried out in a laboratory-scale hot air dryer operating at 50 °C and an air velocity of 2 m/s. Eight apple slices for each experiment were placed on a perforated tray to ensure uniform exposure to the drying air. Microwave (MW) pre-treatments were applied prior to hot air drying to assess their effect on drying kinetics. A domestic microwave oven (maximum output power 700 W) was used, with exposure times of 1 min and 3 min. The MW pre-treatments with 700 W of power for 1 min, and 3 min were chosen because by the test experiments it was concluded that this power output and exposure time are the most suitable for the samples' mass, since MW energy absorption strongly depends on thickness and load. Immediately after the MW treatment, the slices were transferred to the hot-air dryer and dried under the same conditions as the untreated samples. The moisture content of apple slices ($\text{kg}_w/\text{kg}_{\text{dm}}$) was determined gravimetrically at regular time intervals during drying. The moisture ratio (MR) was calculated using the following expression $MR(t) = \frac{M_t - M_{eq}}{M_0 - M_{eq}}$, where M_t is the moisture content at time t , M_0 is the initial moisture content, and M_{eq} is the equilibrium moisture content.

3.3 Numerical modeling of moisture diffusion

Drying kinetics was simulated as one-dimensional moisture diffusion across the slice thickness, based on Fick's second law with Robin-type boundary conditions (see Section 2). The following assumptions were applied:

- Moisture transport occurred only in the axial direction, justified by the condition $L \ll R$.
- Shrinkage was considered negligible in thickness but accounted for in diameter.
- The equilibrium moisture content was determined experimentally for each drying condition.

3.3.1 Crank–Nicolson scheme

The partial differential equation was solved using the *Crank–Nicolson finite difference* method, which is second-order accurate in space and time, and is unconditionally stable. The slab half-thickness was discretized with 150 spatial nodes, and symmetry was imposed at the mid-plane. The *Robin* boundary condition applied at the slab surface allowed simultaneous modeling of internal diffusion (described by D_{eff}) and external convection (characterized by k_e) defined in Equation (2). Figure 1 presents the workflow for numerical modeling of drying curves, including data input, Crank–Nicolson solver, fitting procedure, and post-processing.

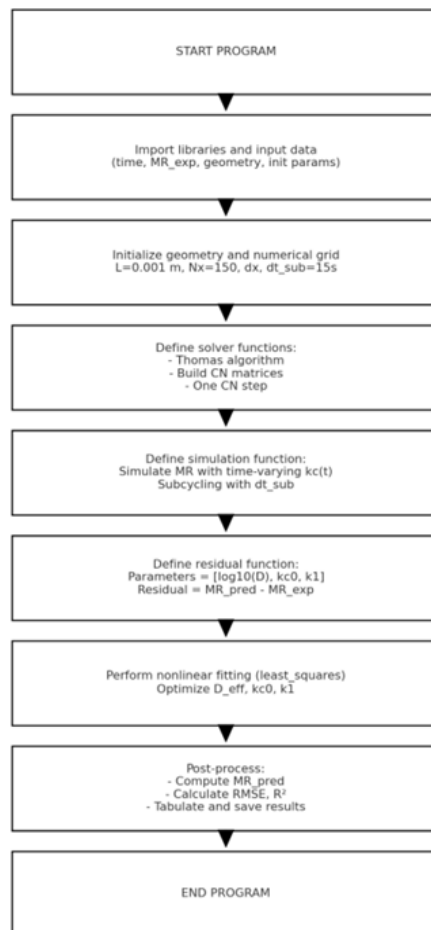


Figure 1. Workflow for numerical modeling of drying curves, including data input, Crank–Nicolson solver, fitting procedure, and post-processing.



3.3.2 Parameter estimation

The effective diffusivity (D_{eff}) was assumed constant, while the surface mass transfer coefficient (k_c) was allowed to vary with time to account for evolving surface characteristics (e.g., pore formation, microstructural collapse). A linear time-dependent expression was used: $k_c(t) = k_{c0} + k_1(t/t_{max})$ where k_{c0} is the initial surface coefficient, k_1 is the rate of change, and t_{max} is the total drying time. The time-averaged surface coefficient over the drying period is given by:

$$\bar{k}_c = \frac{1}{t_{max} \int_0^{t_{max}} k_c(t) dt} = k_{c0} + \frac{k_1}{2} \quad (4)$$

The model was fitted to the experimental MR data using nonlinear least-squares regression, treating D_{eff} , k_{c0} , k_1 as adjustable parameters [13]. The quality of the fit was evaluated using the root mean square error (RMSE) and the adjusted coefficient of determination (R^2_{adj}).

4. RESULTS AND DISCUSSION

4.1. Air drying of apple slices at 50 °C

The drying behavior of untreated apple slices was accurately simulated using the 1-D diffusion model with a time-varying surface mass transfer coefficient (k_c). The model was fitted to the experimental moisture ratio (MR) data by nonlinear least squares regression, with D_{eff} , k_{c0} and k_1 as free parameters, while the initial and equilibrium moisture contents ($M_0 = 7.34 \text{ kg}_w/\text{kg}_{dm}$, $M_{eq} = 0.20 \text{ kg}_w/\text{kg}_{dm}$) were fixed.

The optimized parameters were $D_{eff} = 9.74 \times 10^{-7} \text{ m}^2/\text{s}$, $k_{c0} = 1.20 \times 10^{-7} \text{ m/s}$, and $k_1 = 5.76 \times 10^{-7} \text{ m/s}$ (Table 1). The model showed excellent agreement (Figure 2) with the experimental data ($R^2_{adj} = 0.996$, RMSE = 0.0198).

Table 1. Drying simulation parameters

Drying Case	$D_{eff} \times 10^{-7}$ (m^2/s)	$k_{c0} \times 10^{-7}$ (m/s)	$k_1 \times 10^{-7}$ (m/s)	Bi, avg $\times 10^{-4}$	$Bi_0 \times 10^{-4}$	$Bi_f \times 10^{-4}$	RMSE	R^2_{adj}	Interpretation
Air drying 50 °C	9.74	1.20	5.75	4.19	1.23	7.14	0.0187	0.996	Diffusion-controlled, k_c increases slightly
Microwave (1 min- 700W) and air drying at 50 °C	9.99	1.88	5.38	4.57	1.88	7.26	0.0115	0.998	Faster drying, moderate k_c increase

Microwave (1
min-700W+2
min-140W)
and air
drying at
50 °C

10.0

1.94

7.02

5.45

1.94

8.96

0.0119

0.998

Stronger k_c
increase, still
diffusion-
controlled

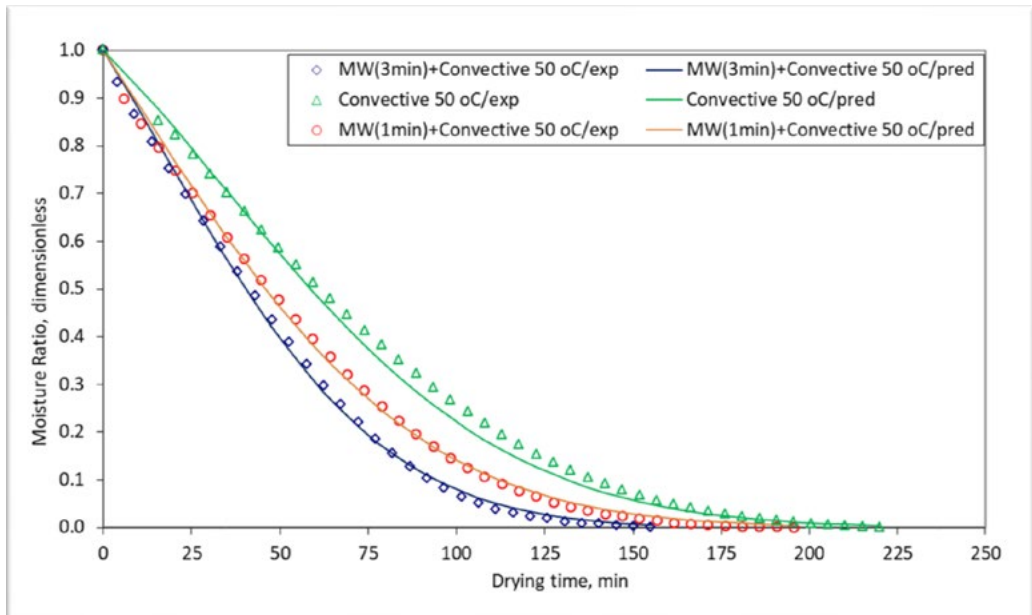


Figure 2. Experimental and simulated drying curves of apple slices: (a) hot-air drying at 50 °C, (b) microwave pre-treatment (1 min) + hot air drying, (c) microwave pre-treatment (3 min) + hot air drying. Symbols represent experimental data; solid lines represent model predictions using constant D_{eff} and time-varying k_c .

The Biot numbers for mass transfer in the slab model ranged between 1.23×10^{-4} (initial) and 7.14×10^{-4} (final) with an average $\bar{Bi} = 4.19 \times 10^{-4}$ (Table 1). These small Biot numbers confirm that moisture transfer was predominantly controlled by internal diffusion within the apple tissue rather than by external convective resistance. Although k_c increased during drying, the Biot numbers remained well below unity ($\ll 1$), reinforcing that the surface resistance played only a minor role.

Reported Biot numbers for fruit and vegetable drying typically range between 10^{-3} and 10^{-1} , depending on product structure, air velocity, and geometry [14]. The estimated diffusivity aligns with literature values for apple tissues dried at moderate temperatures, typically in the range 0.5×10^{-6} – 2×10^{-6} m²/s [14].



4.2. Effect of microwave pre-treatment (1 min)

Microwave pre-treatment (700 W for 1 min) reduced the initial moisture content from $7.34 \text{ kg}_w/\text{kg}_{dm}$ to $M_0=6.65 \text{ kg}_w/\text{kg}_{dm}$. The sample diameter decreased slightly during dehydration (initial radius $R=0.0375 \text{ m}$, final $R=0.0365 \text{ m}$). Moisture ratio data were collected at 41 time points up to 11,742 s. The overall drying caused only limited radial shrinkage ($<7\%$), which supports the earlier assumption that $L \ll R$ and $\tau_z \gg \tau_r$.

The optimized parameters were $D_{eff}=9.99 \times 10^{-7} \text{ m}^2/\text{s}$, $k_{c0}=1.88 \times 10^{-7} \text{ m/s}$, and $k_t=5.38 \times 10^{-7} \text{ m/s}$. The surface mass transfer coefficient increased from $1.88 \times 10^{-7} \text{ m/s}$ to $7.26 \times 10^{-7} \text{ m/s}$ during drying (Table 1). The model closely reproduced the experimental drying curve ($R^2_{adj}=0.998$ and $RMSE=0.0115$), confirming its accuracy across both the early and late stages of drying (Figure 2).

The Biot number was calculated at different stages of drying. It increased from 1.88×10^{-4} (initial) to 7.26×10^{-4} (final), with an average of 4.57×10^{-4} . These low values confirm that drying remained diffusion-controlled, dominated by internal moisture movement rather than by external resistance.

The improvement in drying kinetics compared with untreated slices can be attributed to MW-induced microstructural changes that enhanced surface permeability—consistent with microscopy observations of increased porosity in pre-treated fruits [4], [8]. The Biot numbers observed here are at the low end of typical ranges for fruits and vegetables (10^{-3} – 10^{-1}), which is consistent with the thin geometry and high diffusivity of apple slices at $50 \text{ }^\circ\text{C}$.

4.3 Microwave pre-treatment (3 min)

Sequential microwave pre-treatment at 700 W for 1 min followed by 140 W for 2 min further reduced the initial moisture content to $4.43 \text{ kg}_w/\text{kg}_{dm}$. The slice diameter decreased slightly during drying (initial radius $R=0.0375 \text{ m}$ and final $R=0.0325 \text{ m}$).

The surface mass transfer coefficient k_c increased steadily during drying, reflecting progressive changes in the product surface. It increased from $1.94 \times 10^{-7} \text{ m/s}$ to $8.96 \times 10^{-7} \text{ m/s}$, with an average of $5.45 \times 10^{-7} \text{ m/s}$. These magnitudes are consistent with reported values for apple slices (10^{-7} – 10^{-6} m/s), depending on air velocity and sample geometry [8], [14]. The model provided an excellent description of the experimental drying curves ($RMSE=0.0119$ and $R^2_{adj}=0.998$) seen in Figure 2.

The monotonic increase in k_c with time can be attributed to microstructural phenomena such as cuticle breakdown, pore formation, and surface roughening (case hardening), which collectively reduce external resistance to vapor escape as dehydration progresses. This interpretation agrees with previous microscopy observations of apple tissue showing a more porous surface structure as drying advances.

By contrast, D_{eff} could be adequately represented by a constant value ($\approx 1.0 \times 10^{-6} \text{ m}^2/\text{s}$). This estimate lies within the range reported for apple and similar fruit tissues at $50 \text{ }^\circ\text{C}$ (5×10^{-7} – $2 \times 10^{-6} \text{ m}^2/\text{s}$) [8], [14]. Although some studies employ moisture-dependent D_{eff} formulations that decrease exponentially with decreasing moisture ratio (MR), the present results demonstrate that, for thin apple slices with limited shrinkage, a constant



Deff combined with a time-dependent k_c is adequately reproduces drying kinetics with high accuracy. This finding suggests that surface evolution, rather internal structural change, primarily governs the observed improvement in model accuracy [12].

Biot number calculations further supports this conclusion. Across all cases, Biot numbers remained low, ranging from 1.94×10^{-4} initially to 8.96×10^{-4} at the end of drying (average $\approx 5.45 \times 10^{-4}$). These values, one to two orders of magnitude below unity, indicate that drying was diffusion-controlled, with negligible external resistance. Similar results were reported by [8], who found that thin fruit and vegetable slices exhibit $Biot < 0.01$, while thicker products such as banana slices can reach $Biot \approx 0.1$, indicating greater convective limitation.

Microwave pre-treatment thus accelerated drying primarily by lowering the initial moisture and enhancing surface permeability, without significantly altering D_{eff} [6]. The consistently low Biot numbers ($\approx 10^{-4}$) confirm that drying of thin apple slices at 50°C is governed predominantly by internal moisture diffusion.

The choice between time-dependent and moisture-dependent formulations of transport parameters warrants further consideration. The time-varying k_c approach used here is empirical but provides a realistic way to simulate evolving surface conditions without over-parameterizing the model. In contrast, moisture-dependent diffusivity models are more mechanistic, linking transport resistance to the internal water state. However, they require additional assumptions and may introduce parameter non-uniqueness.

Given the nearly exponential drying curves, the limited radial shrinkage ($0.0375\text{ m} \rightarrow 0.0275\text{ m}$), and the very low Biot numbers, the simpler formulation with constant D_{eff} and time-varying k_c is fully justified. For products with greater structural collapse, such as tomatoes or bananas, moisture-dependent diffusivity models may be necessary to maintain predictive accuracy.

In summary, the present analysis demonstrates that convective air drying of apple slices at 50°C is predominantly governed by internal diffusion, with external resistance decreasing as surface properties evolve. The combination of constant effective diffusivity and time-dependent surface mass transfer coefficient yielded excellent predictive accuracy and physically interpretable results. These findings are in close agreement with international literature and highlight the importance of tailoring diffusion models to the geometry and microstructural behavior of the product under study. The MW pre-treatment reduced drying time at 50°C , by 12% (700 W for 1 min) and 42% (MW combined treatment for 3 min) relative to untreated slices.

5. CONCLUSIONS

This study investigated the convective drying of thin Idared apple slices with and without microwave (MW) pre-treatment, combining experimental data with analytical modeling. A one-dimensional diffusion model with constant effective diffusivity (D_{eff}) and time-varying surface mass transfer coefficient (k_c) accurately described the drying behavior of apple slices under all tested conditions ($R^2_{adj} > 0.996$). The estimated Biot numbers (10^{-4} — 10^{-3}) confirmed that drying of thin apple slices at 50°C was governed



primarily by internal diffusion, with surface resistance contributing only marginally. The effective moisture diffusivity (D_{eff}) was consistently around 1.0×10^{-6} m²/s, in good agreement with literature for apple tissues. The surface mass transfer coefficient (k_c) increased progressively during drying, from approximately 2.0×10^{-7} to 9.0×10^{-7} m/s, reflecting structural modifications at the slice surface. Microwave pre-treatment reduced the initial moisture content and accelerated drying rates, mainly by improving surface permeability. Also, MW pre-treatment reduced drying time at 50 °C, by 12% (700 W for 1 min) and 42% (MW combined treatment for 3 min) relative to untreated slices. However, it did not significantly alter the internal diffusivity of the apple tissue. For thin fruit slices, modeling with constant D_{eff} and time-dependent k_c provides both predictive accuracy and physical interpretability. MW pre-treatment is an effective means of reducing drying time, but the overall drying kinetics remain diffusion-controlled, governed by internal moisture transport.

NOMENCLATURE

Symbol	Definition	Units
M	moisture content (db)	kg _{water} /kg _{dry matter}
M_0	initial moisture content (db)	kg _{water} /kg _{dry matter}
M_{eq}	equilibrium moisture content (db)	kg _{water} /kg _{dry matter}
MR	moisture ratio $(M - M_{eq}) / (M_0 - M_{eq})$	dimensionless
t	drying time	s
t_{max}	total drying time	s
L	half-thickness of the apple slice (slab model)	m
R	slice radius (initial or final, depending on shrinkage)	m
k_c	mass transfer coefficient at the product–air interface	m/s
k_{c0}	initial surface mass transfer coefficient	m/s
k_1	linear coefficient for time-varying surface transfer	m/s
D_{eff}	effective water diffusivity	m ² /s
Bi	Biot number, $k_c L / D_{eff}$	dimensionless
Bi_0	initial Biot number at $t=0$	dimensionless
Bi_f	final Biot number at $t=t_{max}$	dimensionless
\overline{Bi}	average Biot number (over drying period)	dimensionless
τ_z	characteristic drying time in thickness direction	s
τ_r	characteristic drying time in radial direction	s
RMSE	root mean square error (experimental-predicted MR)	dimensionless
R^2_{adj}	adjusted coefficient of determination	dimensionless



References

- [1] B. Llavata, J. V. García-Pérez, S. Simal, and J. A. Cárcel, “Innovative pre-treatments to enhance food drying: a current review,” *Curr. Opin. Food Sci.*, vol. 35, pp. 20–26, 2020, doi: <https://doi.org/10.1016/j.cofs.2019.12.001>.
- [2] J. Dehghannya and M. Habibi-Ghods, “Microwave Drying of Food Materials: Principles, Hybrid Techniques, Modeling Approaches, and Emerging Innovations,” *Compr. Rev. Food Sci. Food Saf.*, vol. 24, no. 6, p. e70312, 2025, doi: [10.1111/1541-4337.70312](https://doi.org/10.1111/1541-4337.70312).
- [3] G. Musielak, M. Mieszczakowska-Frać, and D. Mierzwa, “Convective Drying of Apple Enhanced with Microwaves and Ultrasound—Process Kinetics, Energy Consumption, and Product Quality Approach,” *Appl. Sci.*, vol. 14, no. 3, p. 994, 2024, doi: [10.3390/app14030994](https://doi.org/10.3390/app14030994).
- [4] G. V. S. B. Raj and K. K. Dash, “Effect of intermittent microwave convective drying on physicochemical properties of dragon fruit,” *Food Sci. Biotechnol.*, vol. 31, no. 5, pp. 549–560, 2022, doi: [10.1007/s10068-022-01057-4](https://doi.org/10.1007/s10068-022-01057-4).
- [5] Y. Ma, X. Tian, Y. Wang, H. Zhao, and J. Song, “Comparative Study on Drying Characteristics and Quality of Apple Cubes Dried in Two Different Microwave Dryers,” *Polish J. Food Nutr. Sci.*, vol. 73, no. 4, pp. 367–374, 2023, doi: [10.31883/pjfn/174972](https://doi.org/10.31883/pjfn/174972).
- [6] J. Szadzińska, K. Waszkowiak, and D. Mierzwa, “Hybrid Drying of Apples: A Comparison of Continuous and Intermittent Process Modes,” *Appl. Sci.*, vol. 15, no. 22, p. 12031, 2025, doi: [10.3390/app152212031](https://doi.org/10.3390/app152212031).
- [7] J. Crank, *The Mathematics of Diffusion*, Second edi. Oxford: Clarendon press, 1975.
- [8] M. N. C. Pinheiro and L. M. M. N. Castro, “Effective moisture diffusivity prediction in two Portuguese fruit cultivars (Bravo de Esmolfe apple and Madeira banana) using drying kinetics data,” *Heliyon*, vol. 9, no. 7, Jul. 2023, doi: [10.1016/j.heliyon.2023.e17741](https://doi.org/10.1016/j.heliyon.2023.e17741).
- [9] J. Wu, L. Zhang, and K. Fan, “Recent advances in ultrasound-coupled drying for improving the quality of fruits and vegetables: a review,” *Int. J. Food Sci. Technol.*, vol. 57, no. 9, pp. 5722–5731, Sep. 2022, doi: [10.1111/ijfs.15935](https://doi.org/10.1111/ijfs.15935).
- [10] E. Jakubczyk, K. Rybak, D. Witrowa-Rajchert, A. Wiktor, R. Rąbkowski, and M. Nowacka, “Convective Drying with the Application of Ultrasonic Pre-Treatment: The Effect of Applied Conditions on the Selected Properties of Dried Apples,” *Foods*, vol. 13, no. 23, p. 3893, 2024, doi: [10.3390/foods13233893](https://doi.org/10.3390/foods13233893).
- [11] D. . B. A. G. . K. V. . X. G. Lentzou, “CFD optimization algorithm for a moving boundary problem of isothermal drying and shrinkage,” in *ISHS Acta Horticulturae 1382: VII International Symposium on Applications of Modelling as an Innovative Technology in the Horticultural Supply Chain - Model-IT 2023*, 2023, pp. 41–50.
- [12] T. K. Tepe and F. B. Tepe, “Improvement of pear slices drying by pretreatments and microwave-assisted convective drying method: drying characteristics, modeling of artificial neural network, principal component analysis of quality parameters,” *J. Therm. Anal. Calorim.*, vol. 149, no. 14, pp. 7313–7328, 2024, doi: [10.1007/s10973-024-13280-8](https://doi.org/10.1007/s10973-024-13280-8).



[13] H. S. El-Mesery, A. N. Jibril, A. H. ElMesiry, Z. Hu, X. Zhang, and A. A. Mahdi, "Artificial neural network and machine learning predictive model for assessing physicochemical properties of garlic slices (*Allium sativum* L.) during microwave-assisted convective drying process," *Food Chem. X*, vol. 29, p. 102703, 2025, doi: <https://doi.org/10.1016/j.fochx.2025.102703>.

[14] I. Alibas and A. Yilmaz, "Microwave and convective drying kinetics and thermal properties of orange slices and effect of drying on some phytochemical parameters," *J. Therm. Anal. Calorim.*, vol. 147, no. 15, pp. 8301–8321, 2022, doi: 10.1007/s10973-021-11108-3.

Supplement

```
1. Full numerical Crank–Nicolson fit with time-varying kc written in Python
# New drying case (Meq = 0): 1-D slab CN with time-varying kc(t) = kc0 + k1 * t
/ t_final
# Geometry: thickness = 0.002 m -> L = 0.001 m. Radius shrink 0.0325 -> 0.0275
m (ignored in 1-D z model).
```

```
# Fit parameters: D_eff, kc0, k1. Return full table (4 decimals) and metrics.
```

```
import numpy as np, pandas as pd, time
from scipy.optimize import least_squares
from caas_jupyter_tools import display_dataframe_to_user
```

```
start = time.time()
```

```
# Experimental MR data
t_data = np.array ([0,240,532,824,1117,1409,1701,1993,2285,2577,2870,3162,3454,
3746,4039,4331,4623,4915,5207,5499,5792,6084,6376,6669,6961,7253,7545,7837,8129,84
22,8714,9006,9298], dtype=float)
MR_exp=np.array ([1.0,0.931793478,0.865217391,0.807336957,0.750543478,0.695923
913,0.641304348,0.5875,0.533695652, 0.483695652,0.433152174,0.386413043,0.34076087,0
.296467391,0.256793478,0.218478261,0.183423913,0.153532609,0.125543478,0.102445652,
0.080706522,0.063586957,0.050543478,0.0375,0.02826087,0.021467391,0.017119565,0.011
413043,0.007608696,0.005978261,0.002445652,0.001902174,0.0], dtype=float)
```

```
# Geometry / numerics
L = 0.001 # half-thickness
Nx = 150
dx = L / Nx
dt_sub = 12.0 # smaller substep for accuracy
weights = np.ones(Nx+1); weights[0]=0.5; weights[-1]=0.5; weights = weights / Nx
t_final = t_data[-1]
```



```
# Thomas solver
def solve_tridiagonal(a,b,c,d):
    n=len(b)
    cp=np.empty(n-1); dp=np.empty(n)
    cp[0]=c[0]/b[0]; dp[0]=d[0]/b[0]
    for i in range(1,n-1):
        denom=b[i]-a[i-1]*cp[i-1]
        cp[i]=c[i]/denom
        dp[i]=(d[i]-a[i-1]*dp[i-1])/denom
    dp[n-1]=(d[n-1]-a[n-2]*dp[n-2])/(b[n-1]-a[n-2]*cp[n-2])
    x=np.empty(n); x[-1]=dp[-1]
    for i in range(n-2,-1,-1):
        x[i]=dp[i]-cp[i]*x[i+1]
    return x

def build_ops(D, kc):
    n=Nx+1
    lower=np.zeros(n-1); diag=np.zeros(n); upper=np.zeros(n-1)
    invdx2 = 1.0/(dx*dx)
    for i in range(1,n-1):
        lower[i-1]=D*invdx2
        diag[i]=-2*D*invdx2
        upper[i]=D*invdx2
    diag[0]=-2*D*invdx2; upper[0]=2*D*invdx2
    lower[-1]=2*D*invdx2
    diag[-1]=-2*D*invdx2 - 2*kc/dx
    return lower,diag,upper

def cn_step(C_old, D, kc, dt):
    lower,diag,upper=build_ops(D,kc)
    n=Nx+1
    aM = -0.5*dt*lower.copy()
    bM = 1.0 - 0.5*dt*diag
    cM = -0.5*dt*upper.copy()
    rhs = np.zeros(n)
    rhs[0] = (1.0 + 0.5*dt*diag[0])*C_old[0] + 0.5*dt*upper[0]*C_old[1]
    for i in range(1,n-1):
        rhs[i] = 0.5*dt*lower[i-1]*C_old[i-1] + (1.0 + 0.5*dt*diag[i])*C_old[i] +
0.5*dt*upper[i]*C_old[i+1]
    rhs[-1] = 0.5*dt*lower[-1]*C_old[-2] + (1.0 + 0.5*dt*diag[-1])*C_old[-1]
    C_new = solve_tridiagonal(aM,bM,cM,rhs)
    return C_new
```



```
# simulate with  $kc(t) = kc_0 + k_1 * t / t\_final$  (Meq=0, MR = mean(C))
def simulate_timevary_kc(D, kc0, k1):
    C = np.ones(Nx+1)
    MR_model = []
    t_prev = 0.0
    for t_target in t_data:
        dt_total = t_target - t_prev
        if dt_total <= 0:
            MR_model.append(np.dot(weights, C)); continue
        remaining = dt_total
        while remaining > 1e-12:
            dt = min(dt_sub, remaining)
            t_mid = t_prev + 0.5*dt
            kc_now = kc0 + k1 * (t_mid / t_final)
            kc_now = max(kc_now, 1e-12)
            C = cn_step(C, D, kc_now, dt)
            C = np.maximum(C, 0.0)
            t_prev += dt
            remaining -= dt
        MR_model.append(np.dot(weights, C))
    return np.array(MR_model)

# residuals:  $x = [\log_{10}(D), kc_0, k_1]$ 
def residuals_timevary(x):
    logD, kc0, k1 = x
    D = 10**logD
    pred = simulate_timevary_kc(D, kc0, k1)
    return pred - MR_exp

# initial guess and bounds
x0 = [np.log10(2.0e-8), 2.0e-7, 0.0]
lb = [np.log10(1e-12), 1e-10, -5e-6]
ub = [np.log10(1e-6), 1e-3, 5e-6]

res = least_squares(residuals_timevary, x0, bounds=(lb,ub), xtol=1e-9, ftol=1e-9,
gtol=1e-9, max_nfev=300)

logD_opt, kc0_opt, k1_opt = res.x
D_opt = 10**logD_opt
MR_pred = simulate_timevary_kc(D_opt, kc0_opt, k1_opt)

# metrics
diff = MR_exp - MR_pred
```



ISAE 2025 - Book of Abstracts
The 7th International Symposium on Agricultural Engineering

```
RMSE = np.sqrt(np.mean(diff**2))
MAE = np.mean(np.abs(diff))
ss_res = np.sum(diff**2)
ss_tot = np.sum((MR_exp - np.mean(MR_exp))**2)
R2 = 1 - ss_res/ss_tot
npts = len(MR_exp); p = 3
R2_adj = 1 - (1 - R2) * (npts - 1) / (npts - p - 1)

# Table rounded
df = pd.DataFrame({'Time_s': t_data, 'MR_exp': np.round(MR_exp,4), 'MR_
pred': np.round(MR_pred,4)})
display_dataframe_to_user("Case 3: MR_exp vs MR_pred (time-varying kc,
Meq=0)", df)

print("Fit complete (time-varying kc, Meq=0).")
print(f"D_eff = {D_opt:.6e} m^2/s")
print(f"kc0 = {kc0_opt:.6e} m/s")
print(f"k1 = {k1_opt:.6e} m/s (over t_final scale)")
print("Metrics:")
print(f"RMSE = {RMSE:.6g}, MAE = {MAE:.6g}, R2 = {R2:.6g}, R2_adj = {R2_
adj:.6g}")
print("Elapsed: {:.1f} s".format(time.time()-start))
```